NON-RELATIVISTIC AND RELATIVISTIC ELECTRONICS

DETERMINATION OF DISCHARGE GAP CONDUCTION IN THE PLASMA SWITCH

E.I. Skibenko, A.N. Ozerov, V.B. Yuferov
National Science Center "Kharkov Institute of Physics and Technology", Kharkiv, Ukraine
E-mail: skibenko38@gmail.com, ozerov@kipt.kharkov.ua

Operational analysis and the obtained results are presented for nanosecond pulsed current/voltage generators involving use of plasma switches, shortly PCS-PCI. The electrical conduction in the plasma-filled discharge gap was determined by calculations versus the plasma electron temperature, the concentration of multicharged ions and their ionization state number. Some factors affecting the conduction value of the PCS-PCI discharge gap have been established, such as the cross-section for electron scattering by the intrinsic atomic field and the electron-neutral collisions, which lead to early reduction in the PCS-PCI discharge-gap conduction before the onset of the current cut off phase.

PACS: 52.25.Jm; 52.50.Dg; 41.75.Ak

INTRODUCTION

The challenge of nanosecond power engineering is to create the devices for obtaining power up to 10^{14} W, voltage up to 10^6…10^7 V, and current up to 10^6 A. The range of applicability of the developments is rather wide and diversified. It involves: the investigation of the rate of electric discharge development in solids, liquid and gaseous dielectrics; high-speed photography for studying ultrafast processes in plasma; radiolocation as it pertains to precision radar ranging; high-speed X-ray dosimetry in the field of ballistics and explosion physics; creation of spark/streamer chambers for nuclear physics research; powerful pulsed solid-state/gaseous lasers; high-power nanosecond electron accelerators.

One of the main directions for the development of pulsed energetics and high-power electronics [1 - 6] is represented by systems with inductive energy storage units and plasma switches. Their use enables one to increase the power of pulsed generators, to reduce the pulse duration, to create compact pulsed generators and electron accelerators. In brief, the sequence of the PCS-PCI operation can be described as follows. Close to the pulsed generator load, the plasma jumper is formed between the earth and potential electrodes (e.g., between the anode and the cathode). As the current flows in the bridge, a partial or complete capacitive-to-inductive storage-energy transfer takes place. On reaching certain conditions, the plasma jumper conduction sharply decreases, this being accompanied by the occurrence of anomalous resistance. As a result, the vortex EMF is generated, and the energy stored in the inductor is switched to the load. The plasma-filled diodes, developed by A.A. Plyutto when investigating the processes of powerful electron beam generation and collective ion acceleration [7, 8], can be considered as the PCS-PCI prototypes. Table 1 gives the list and parameters of the experimental facilities [9 - 16] created and investigated during the period of 1976 to 1995. The following notation was introduced:

$\frac{d}{dt}$ – rates of current, voltage, resistance rise, respectively, (I, U, R), A/s, V/s, Ω/s;
n_p – plasma density, cm^{-3};
$\Delta t_{c.c.}$ – period closed circuit PCS-PCI, s;
Δt_{cutoff} – current cutoff phase duration, s;
W_0 – plasma-free diode power, W;
W – plasma-filled diode power, W;
k – coefficient of energy transfer to the load, %;
MG – Marx generator and its parameters Q, I_0, U_0, L, C;
N – number of plasma sources (plasma guns);
d_k – cathode diameter (internal electrode), mm;
d_a – anode diameter (external electrode), mm;
H – magnetic field strength, kOe;
$\frac{U}{U_0}$ – voltage multiplication factor;
$\frac{dR}{dt}$ – rate of PCS-PCI resistance rise at the moment before the current cutoff, Ω/s;
R_{cutoff} – PCS-PCI resistance at current cutoff, Ω;
I_{cutoff} – total current at the moment of cutoff, A;
U_{cutoff} – PCS-PCI voltage, kV or MV;
I_L – load current at the moment of peak power, A;
Q – energy content, MJ.

Table 1

Experimental facilities and their parameters

Facilities	Parameters, results	References, year
Proto-1 accelerator	$\frac{dI}{dt} = 3 \cdot 10^{13}$ A/s, $\frac{dU}{dt} = 10^{15}$ V/s, n_p=10^{12}…10^{13} cm^{-3}, I_{cutoff}=75 kA, Δt_{cutoff}=$5 \cdot 10^{-9}$ s	[9, 10] 1976-1977
Python accelerator	I_{cutoff}=10^3 кА	[11] 1981
Gamble-1 pulse generator	$\Delta t_{c.c}$=10^{-7} s, Δt_{cutoff}=10^{-8} s	[12] 1983

<table>
<tr><td>Gamma accelerator</td><td>W_0=5·10^{10} W, W=3·10^{11} W, I_{cutoff}=200 kA, Δt_{cutoff}=3·10^{-7} s, k=60%</td><td>[13]
1986</td></tr>
<tr><td>Marina
Pulse generator</td><td>$\frac{dI}{dt} = 1.2 \cdot 10^{13}$ A/s, $\frac{dR}{dt} = 10^{9}$ Ω/s, R_{cuttof}=16 Ω, n_p=10^{14} cm^{-3}, U_0=700 kV,
U=2.5 MV, $\frac{U}{U_0} = 3.57$, I_{cuttof}=280 kA, I_L=135 kA, k=48.2%</td><td>[6, 14]
1985
1987</td></tr>
<tr><td>GIT-4</td><td>4 MG, Q=2.16 MJ, L=0.1 μH, C=4.8 μF:
1. Liner experiment mode: N=64, d_A=560 mm, d_C=480 mm, U_0=720 kV, I_{cutoff}=2.8 MA, I_L=2.4 MA, k=85.7%, H=23.1 kOe;
2. Two-way plasma injection mode: radially and along the z-axis (axially). In the z-axis case, the pulse parameters are better. For the cathode 160 mm in diameter, they are: R_{cutoff}=1 Ω, I_{cutoff}=1.65…1.75 MA, W=2 TW, U_{cutoff}=1.5 MV. For conically shaped cathode: R_{cutoff}=2.3…3 Ω, I_{cutoff}=1 MA, W=3 TW, U_{cutoff}=3 MV;
3. The two-step circuit mode (with two PCIs). 1st step: d_C=280 mm, d_A=350 mm – squirrel wheel, N=64. 2nd step: – coaxial d_{ext}/d_{int}=210/40 mm, N=32. The voltage multiplication factor $\frac{U}{U_0} \sim 13$ is obtained at U_0=480 kV, U=6 MV</td><td>[15]
1990</td></tr>
<tr><td>HAWK</td><td>MG: U_0=640 kV, I_0=720 kA, Q=225 kJ, C=1 μF. Plasma sources with surface breakdown, or 12 coaxial guns in the form of coaxial cable cuts, or 4 gas-charging valves (H_2, Ar, He) with capacitor breakdown. n_p=10^{15} cm^{-3}. Diode tube as a load
<table>
<tr><td>d_C, mm</td><td>U_{cutoff}, MV</td><td>I_{cutoff}, kA</td><td>I_L, kA</td><td>R_L, Ω</td><td>W, TW</td><td>k, %</td></tr>
<tr><td>100</td><td>0.9</td><td>635</td><td>500</td><td>1.5</td><td>0.4</td><td>78.74</td></tr>
<tr><td>50</td><td>1.2</td><td>500</td><td>400</td><td>3</td><td>0.5</td><td>80</td></tr>
<tr><td>cone</td><td>1.6</td><td>600</td><td>465</td><td>4</td><td>0.7</td><td>77.5</td></tr>
<tr><td>26</td><td>2.0</td><td>500</td><td>250</td><td>7</td><td>-</td><td>50</td></tr>
</table></td><td>[16]
1992</td></tr>
<tr><td>DI</td><td>Diagnostic aids: Rogowski coils, capacitive divider, microwave interferometers on a frequency of 35 GHz, X-ray detectors:
N=1; 4; 12. $n_p \geq 1.7 \cdot 10^{13}$ cm^{-3}, $\frac{U}{U_0} average = 7.5$, $\frac{U}{U_0} \max = 10...12$.
U_{cutoff}=360 kV, I_L=140 kA, Δt=30 ns, mass: 315 kg</td><td>[17]
1989-1995</td></tr>
<tr><td>DIN-2K</td><td>U_{cutoff}=300 kV, I_L=100 kA, Δt=20…30 ns</td><td>[18]
1998</td></tr>
</table>

The main mechanism of plasma current switch (interrupter) operation relies on the anomalous resistance effect, which arises at the instability of plasma having the current density higher than a certain critical value [19]. In this case, if the cause of the instability is the excess of the critical current value, then the increase in the instability should give rise to the mechanism that would limit the increase in the current. In other words, there should appear an additional, the so-called anomalous resistance. This physical phenomenon has been investigated by two groups of physicists from the Kurchatov Institute for Atomic Energy and the KIPT, and was registered as a discovery No 112 in 1972 [20]. Table 2 gives the instabilities arising at the critical current excess. Note that for the experiments with the PCS-PCI it is of importance to know the resistance value at both the linear and turbulent stages of interaction. As indicated in refs. [14, 15, 21], the process of current diffusion (flow) is going on for about 800 ns of the conduction phase, this attesting to the constancy of the average value of $\sigma \cdot l = const$, where l is the plasma sheet thickness, σ is the plasma conductivity.

Table 2

Electric-current plasma instabilities relating to the anomalous resistance problem

Instability type	Instability threshold	Frequency	Increment of growth
Buneman instability	$u_0 > \vartheta_{te}$	$\sim \omega_{pi}$	$\sim \omega_{pi}$
Ion-acoustic instability	$u_0 > \left(\frac{T_e}{m_i}\right)^{\frac{1}{2}}$	$\leq \omega_{pi}$	$\leq \frac{\omega_{pi} u_0}{\vartheta_{te}}$
Electrostatic modes $k_\perp^2 >> k_z^2$	very low, sometimes < ϑ_{ti}	$\ll \omega_{He}$	$\sqrt{\omega_{He}\omega_{Hi}}$

Here u_0 is the electron drift velocity; ϑ_{te} is the electron thermal velocity; ω_{pi} is the ion plasma frequency; T_e is the electron temperature; m_i is the ionic mass; ω_{Hi} is the ion cyclotron frequency.

The Buneman instability is the excitation of longitudinal electrostatic plasma oscillations at the rate of increase of about the ion plasma frequency. In this case, the initial electron/ion distribution functions take the form of two δ-functions shifted relative to each other by the average velocity u_0 value. In the ion-acoustic instability case, the oscillations arise at the electron drift velocities u_0 lower than the thermal velocities. In the order of magnitude, the growth rate of ion-acoustic oscillations is the ion plasma frequency reduced in the electron drift-to-thermal velocity ratio. At $u_0 \to \vartheta_{te}$, the ion-acoustic instability passes into the Buneman instability. In the anomalous resistance problem, the class of instabilities relative to electrostatic perturbations, $k_\perp^2 >> k_z^2$, may play an important role. These are the waves, where the wave vector component along the magnetic field is considerably less than the transverse component of the wave vector, and the frequencies are substantially lower than the electron Langmuir frequency.

For a more complete understanding and analysis of the process of current switching in the PCS-PCI facilities, it makes sense to trace the role of the so-called influence factors essentially responsible for the operational efficiency of these devices (Table 3).

Table 3

Influence factors [1-23] responsible for the current-switching operational efficiency in the PCS-PCI facilities

Influence factors	Facilities						
	Proto-1	Python	Gamble-1	Gamma	Marina	GIT-4	HAWK
Cathode diameter, d_c	$I_{PCI}=f(d_c)$ has the most clearly defined character and is determining in the current change by the order of magnitude				$\frac{I_{cutoff}}{d_k} = 7...8 = const$, kA/mm		
Number of plasma guns, N	The current amplitude changes as a function of the plasma density, $I_{cutoff} \sim N^{0.5}$					$I_{cutoff} \sim N^{0.5}$	$I_{cutoff} \sim N^{0.25}$
Time delay between pulses of plasma and current, Δt_{del}	The minimum delay corresponds to the time required for crossing the plasma interelectrode gap. The maximum delay corresponds to the attainment of the saturation current						
Rate of current rise $\frac{dI}{dt}$	With increase in the rate of current injection $\frac{dI}{dt}$ the limiting current amplitude increases, and the duration of conduction phase decreases						
Constancy of the product $\sigma \cdot l = const$	Σ – plasma conductivity, l – plasma layer thickness						
Plasma composition	Switching characteristics get improved in R and $\frac{U}{U_0}$ values by factors 2 to 2.5 with decrease in the atomic mass of plasma ions (H_2, D_2; Ar, Kr) [16]						
Operation modes and polarity of electrodes	Internal electrode (cathode) polarity reversal (from "-" to "+") leads to considerable drop in the characteristics of the current cutoff phase. At the "-" mode, $\frac{dR}{dt} = 5...8 \cdot 10^8$ Ω/s, at the"+" mode $\frac{dR}{dt} \to 5 \cdot 10^7$ Ω/s						
Direction of plasma injection	Plasma injection from the cathode side towards the anode reduces the expenditure of energy for plasma creation by order of magnitude in contrast with plasma injection from the anode side						

For our purpose and considering the physics of the process, the PCS-PCI performance can be divided into two stages (phases) and several steps. The first stage of the process represents the conductivity phase that includes the following steps: 1) plasma injection, 2) filling of the discharge gap with plasma, 3) current increase, 4) stabilization of the plasma dynamic characteristics (density, temperature, elemental composition) in the discharge gap of the PCS-PCI. The second stage of the process represents the current cutoff phase. The PCS-PCI conduction phase is first of all responsible for the efficiency of energy transfer from the capacitive storage to the inductive one. The main characteristics of the conduction phase involve the initial PCS-PCI impedance, the peak current amplitude, the discharge gap conduction. The current cutoff phase is decisive (resulting) phase in the PCS-PCI work. Its major characteristic is the rate of impedance change of the switch at its opening.

So, the goal of the present investigation has been to determine the discharge gap conduction of the PCS-PCI versus the following plasma parameters: electron temperature (energy), plasma composition, ionization state distributions of plasma particles, average charge of the plasma.

1. DETERMINATION OF PCS-PCI DISCHARGE-GAP PLASMA PARAMETERS

1.1. ANALYTICAL EXPRESSIONS

According to ref. [24], the plasma conduction is expressed by:

$$\sigma = \frac{ne^2\tau_e}{m_e}, \quad (1)$$

$$\tau_e = \frac{3\sqrt{m_e}\,(KT_e)^{\frac{3}{2}}}{4\sqrt{2\pi}\cdot n\Lambda e^4} = 3.44\cdot 10^5 \frac{T_e^{\frac{3}{2}}}{n\Lambda}, \quad (2)$$

where n is the plasma density; τ_e is the collision time; T_e is the electron temperature; K is the Boltzmann constant; m_e is the electron mass; e is the electron charge; Λ is the Coulomb logarithm.

The conduction is independent of the plasma density, and rapidly increases with T_e increase. Note that this is of importance when choosing the type of the plasma source for filling the PCS-PCI discharge gap. Formula (1) is applicable for fully ionized plasma having singly charged ions. The presence of multicharged ions considerably reduces the plasma conduction. At plasma ionic component concentrations with charges z_1, z_2, … equal to a_1, a_2, … , formula (1) for σ should be replaced by the following expression [19]:

$$\sigma \approx 10^7 \left(\frac{\Sigma a_k z_k}{\Sigma a_k z_k^2} \right) \cdot T_e^{\frac{3}{2}}. \quad (3)$$

For the plasma with a high electron temperature, formula (3) may undergo the following changes. For the fast electron, the effective scattering cross-section σ_{ei} at a too high ionic charge becomes substantially lower than the geometrical cross-section of the ion. Meanwhile, the interaction of the electron with the intrinsic atomic field becomes to play a substantial role in the process of scattering. As a result of this, the scattering cross-section considerably increases in comparison with the value obtained when the ion is presented as a point charge. At rather high electron energies, the effective electron scattering cross-section will be determined no longer by the ionic charge z_i, but by the atomic number z_a, increasing in proportion to z_a^2. In the intermediate energy range, where the relationship $\sigma_{ei} \sim z_i^2$ changes to $\sigma_{ei} \sim z_a^2$, the effective scattering cross-section decreases slower than $1/T_e^2$. For this reason, the conduction of high-temperature plasma, having heavy components, increases slower than by the $T^{3/2}$ law, and it appears very sensitive even to a small portion of impurities. For example, in the hydrogen plasma at $T_e \sim 10^{-4}$ eV the contribution of a single Hg atom or ion to the process of electron deceleration is several thousand times higher than the contribution of the hydrogen ion. In weakly ionized plasma, formula (3) is yet invalid if the electron-neutral collisions are more frequent than electron-ion collisions. In this case, one should turn back to expression (1) for conduction, and replace τ_{ei} with τ_{en} that denotes the average time of electron collisions with neutrals and molecules [19]:

$$\sigma = \frac{ne^2\tau_{en}}{m_e}, \quad (4)$$

The temperature behavior of the conductance coefficients of this plasma will depend on the behavior of the effective electron-neutral scattering cross-section. However, in the weakly ionized plasma it is the degree of ionization that is the factor, which determines the temperature dependence. Indeed, $\tau_{en} \sim 1/n_0$, therefore σ is proportional to the n/n_0 ratio. Hence, at moderate temperatures ($T \ll 1$) σ is proportional to a drastically varying exponential factor *exp(-1/2T)*.

As a result, we give one of the conclusions of theoretic treatment for the current-carrying capability of plasma under the electric field, namely that at high plasma density and a relatively low electric field intensity the experimentally measured plasma conduction values are in agreement within the experimental error with the values calculated by formula (3) [19].

1.2. CALCULATION DATA ON PCS-PCI DISCHARGE GAP CONDUCTION

The electrical conduction σ of the discharge gap filled with singly ionized plasma was calculated by eqs. (1) and (2) versus the electron temperature T_e. The calculation data are presented in Fig. 1.

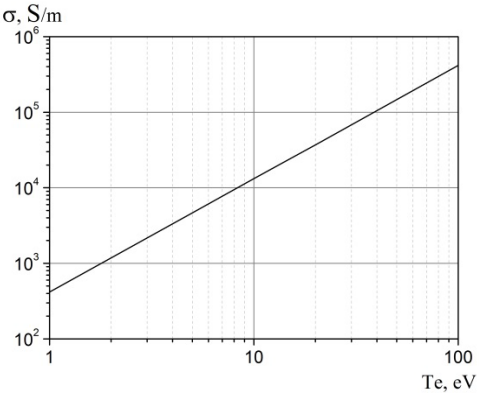

Fig. 1. Plasma conduction in the PCS-PCI discharge gap versus electron temperature

The range of σ variation extends from $4\cdot 10^2$ s to $4\cdot 10^5$ s with T_e ranging from 1 to 100 eV. In actual practice, it is seldom that the ions of well-ionized plasma, except the hydrogen plasma, occur to be singly charged ($k >> 1$). To make the estimations of σ correspond more to real conditions, we here consider the case of argon plasma [25] with the degree of ionization close to 100%; it contains multiply ionized ions with the ionization states up to k=10. Table 4 lists the argon-atom ionization potentials of different ionization multiplicity [26].

Table 4

Argon-atom ionization potentials of different ionization multiplicity

k	1	2	3	4	5	6	7	8	9	10	11
E_i,eV	15.75	27.62	40.90	59.69	75.0	91.3	123.9	173.4	422.6	479.0	539.0

The ion density in each ionization state can be estimated by solving the following set of equations [27]:

$$n_e = \sum\nolimits_k N_{ik} \cdot k, \quad (5)$$

$$N_{ik} = N_{i,k-1} \cdot \frac{t_0^k}{\tau_{ik}}, \quad (6)$$

$$\tau_{ik} = \frac{1}{n_e \langle \sigma v \rangle_{ik}} = \frac{1}{n_e \cdot S_{ik}}, \quad (7)$$

where N_i is the ion density, n_e is the density of plasma electrons, S_i is the rate of atom ionization by electron impact, the k index denotes the number of ionization state, t_0^k is the characteristic time, within which the plasma particle ionization is possible, and the electron temperature is at its maximum, τ_{ik} is the time of electron-impact ionization. The N_{ik} value was calculated on the assumption that the lifetime t_0^k of ions of different charges is the same, and is determined by the characteristic time of the process under consideration; in this instance it is around the time of filling the discharge gap with plasma, i.e., ~10^{-5} s. The data calculated for the initial argon plasma density of $1 \cdot 10^{14}$ cm^{-3}, electron temperature of 100 eV, are given in Fig. 2. It can be seen that the ion density in the k=6 ionization state exceeds the particle density in any other state.

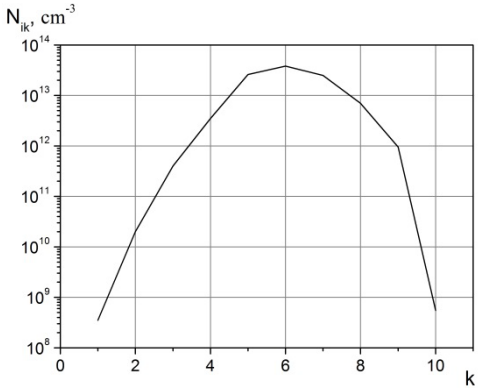

Fig. 2. Ionization state distribution of multicharged ion concentration in Ar well-ionized plasma of density 10^{14} cm^{-3} and T_e=100 eV

The average charge of plasma particles is calculated by the formula

$$\bar{z} = \frac{\sum_k N_{ik} \cdot z_{ik}^2}{\sum_k N_{ik} \cdot z_{ik}}, \quad (8)$$

and is found to be $\bar{z} = 6.25$. It is of interest to estimate the ionization losses and to compare the calculation data with the energy of plasma devices (sources) realizing the plasma filling of the discharge gap. The ionization losses are given by the expression [28].

$$\frac{dE}{dt} = E_{ik} N_{ik} N_e S_{ik}, \quad (9)$$

where E_i is the ionization potential (see Table 4). With allowances made for the multicharged ion densities, ionization power losses were calculated, the variations of which with a growing degree of ionization, are presented in Table 5.

Table 5

Ionization power losses at increasing degree of ionization

k	4	5	6	7	8
$\frac{dE_{ik}}{dx}$, kW	0.8	14.5	35.5	9.5	0.5

The total ionization losses are amount to about 60 kW and stay within the limits of the energy store of plasma-gun power supply sources.

With due regard for the data of Fig. 2 and eq. (3), we calculate the electric conduction of the plasma-filled discharge gap as a function of the ionization state number (Fig. 3). As k changes from 1 to 10, σ decreases by nearly an order of magnitude. A relatively more rapid decrease in σ is observed in the range of k variation from 1 to 6…7. At $k \approx 6…7$, the change in σ is insignificant, because in this range the multicharged ion density decreases by several orders of magnitude. It is of interest to estimate the rate of σ decrease in several special cases discussed below.

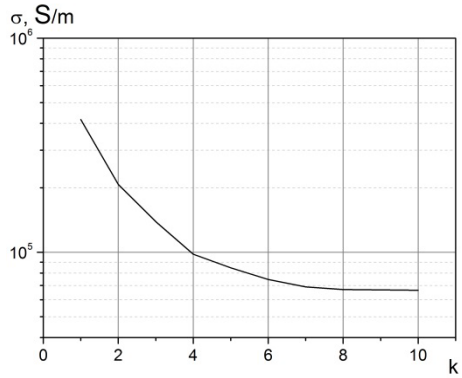

Fig. 3. Electric conduction of the discharge gap versus the ionization state number of multicharged ions in Ar plasma of density 10^{14} cm^{-3} and T_e=100 eV

1.2.1. SPECIAL CASES

1. This is the case of the plasma having a very high electron temperature, when the electron-intrinsic atomic field interaction starts to play a substantial role, i.e., the effective electron scattering cross-section is determined not by the ion charge z_i, but by the atomic number z_a. It increases in proportion to z_a^2, and hence, decreases σ. So, for argon we have $z_a^2 = 18^2 = 324$.

2. The second case refers to weakly ionized plasma, when electrons collide more often with neutrals than with ions, i.e., $\nu_{en} > \nu_{ei}$. Here, the σ value is yet calculated by formula (4). At electron-neutrals collision frequencies (Ar, density of 10^{13} cm^{-3}) $\nu_{en} \geq 5 \cdot 10^{-4}$ s^{-1} for T_e=100 eV, the σ value begins to decrease.

2. DISCUSSION OF RESULTS. CONCLUSIONS

1. At themomentofcurrent cutoff, the final resistance of PCS-PCI consists of three components. The first component, R_0, is determined by the initial electrical conductance of the plasma-prefilled discharge gap. At that, the plasma should meet some parametric requirements such as the density of ~10^{14}…10^{15} cm^{-3}, electron temperature of ~ 100 eV, high degree of ionization (close to 100%), low content and arrival of neutrals, the absence or low content of multicharged ions. The initial R_0-values may range widely from 10^{-6} Ω to several tenths of ohm, so that in the extreme case it may reduce the rate of PCS-PCI resistance increase, thereby

limiting other PCS-PCI parameters. The second component, $\left(\frac{dR}{dt}\cdot\Delta t\right)$, may cause the increase in the PCS-PCI resistance, $R_{PCS\text{-}PCI}$, up to several Ohms (ten at the utmost). The third component, R_{turb}, is of the order of several Ohms. In the "MARINA" generator experiment, the total final resistance was registered to be 16 Ohm [6, 14].

2. The experience in working with the PCS-PCI pulsed generators shows that to provide reliable plasma filling of the discharge gap in compliance with the specified requirements, it is essential that plasma sources of different types (duplicating and complementing each other) should be used, e.g., the sources with dielectric surface breakdown, coaxial plasma guns, pulsed inlet of gas or gases having low atomic number (H_2, D_2, He), much like in the HAWK facility [16]. Besides, the optimum variant of filling the discharge gap with plasma appears to be the method providing the homogeneity of plasma, i.e., it excludes its multicomponent content.

3. The above-mentioned plasma sources for filling the discharge gap meet the specified requirements as to the plasma amount and its density, but they differ in the plasma composition parameter. The plasma guns with the dielectric surface breakdown generate plasma, the heavy particles of which represent polyatomic molecules and ions. The characteristic property of this molecular plasma is the presence of inelastic collisions that give rise to a change of rotational and vibrational state of the colliding particles [26, 29]. In the general case, the partially ionized plasma *(*< 100%) exhibits a wide variety of inelastic processes. In parallel with excitation of rotational and vibrational degrees of freedom of molecules and molecular ions, there also occur the processes of dissociation, electron excitation, ionization and recombination as well as the related processes of emission and absorption of radiation. The last-mentioned group of processes plays a decisive role in establishing the electron concentration level and electron temperature in the plasma, this being due to the vital role of the corresponding terms (dependent on the inelastic collision cross-sections) in the continuity/energy equations for electrons. At that, given the inelastic processes, careful consideration should be given to the derivation and choice of the conservation equations for electrons, and also, the equations for the rate of processes responsible for the population of different atomic excitation levels. All of this may place certain restrictions on the use of the plasma sources with the dielectric surface breakdown for filling the PCS-PCI discharge gap. It is of particular importance to take this into account as the need arises to upgrade the parameters towards increasing MV, MA, MJ, TW.

REFERENCES

1. G.A. Vorob'yov, G.A. Mesyats. *The technique of high-voltage nanosecond pulse formation*. M.: "Gosatomizdat", 1963.
2. G.A. Mesyats, A.S. Nasibov, V.V. Kremnev. *Generation of high-voltage nanosecond pulses.* M.: "Ehnergiya", 1970.
3. G.A. Mesyats. *Generation of high-power nanosecond pulses.* "M.: "Sov. Radio", 1974.
4. B.M. Koval'chuk, V.V. Kremnev, Yu.F. Potalitsin. *High-current nanosecond switches. Executive editor G.A. Mesyats.* Novosibirsk: "Nauka", 1979.
5. V.V. Kremnev, G.A. Mesyats. *Methods of pulse multiplication and transformation in high-current electronics.* Novosibirsk: "Nauka", 1987.
6. B.M. Koval'chuk, G.A. Mesyats. High-power nanosecond pulse generator with a vacuum line and plasma interrupter // *Doklady AN SSSR*, 1985, v. 284, № 4, p. 857-859 (in Russian).
7. K.V. Suladze, B.A. Tskhakaya, A.A. Plyutto. Peculiarities of intense electron beam formation in bounded plasma // *Pis'ma v ZhEhTF*, 1969, v. 10, iss. 6, p. 282-285 (in Russian).
8. G.P. Mkheidze, A.A. Plyutto, E.D. Korop. Ion acceleration at current flow through plasma // *ZhTF*. 1971, v. 41, iss. 5/6, p. 952-963.
9. C.W. Mendel, S.A. Goldstein, P.A. Miller. The plasma erosion switch // *Proc. I IEEE Pulsed power conf. (PPC).* Lubbock, 1976, p. 1c2-1-c2-6.
10. C.W. Mendel, S.A. Goldstein, P.A. Miller. A fast opening switch for use in REB diode experiments // *J. Appl. Phys*. 1977, v. 48, № 3, p. 1004-1006.
11. R. Stringfield, R. Schneider, R.D. Genuario, et al. Plasma erosion switch with imploding plasma loads on a multi-terawatt pulsed power generator // *J. Appl. Phys.* 1981, v. 52, № 3, p. 1278-1284.
12. R.A. Meger, R.F. Commisso, G. Coopersteinet, et al. Vacuum inductive store pulse compression experiments on a high power accelerator using plasma opening switches // *Appl. Phys. Lett*. 1983, v. 42, p. 943-945.
13. Eh.N. Abdulin, G.P. Bazhenov, A.A. Kim, et al. Plasma current interrupter at microsecond times of energy input into the inductive storage // *Fizika Plazmy*. 1986, v. 12, iss. 10, p. 1260-1264 (in Russian).
14. G.A. Mesyats, S.P. Bugaev, A.A. Kim, et al. Microsecond plasma opening switches // *IEEE Trans. Plasma Sci.* 1987, v. 15, № 6, p. 649-653.
15. B.M. Kovalchuk, G.A. Mesyats. Superpower pulsed systems with plasma opening switches // *Proc. VIII Intern. Conf. on High-Power Particle Beam Research and Technology.* Novosibirsk, 1990, v. 1, p. 92-103.
16. P.F. Goodrich, D.D. Hinchelwood. High-power opening switch operation on "HAWK" // *Proc. IX IEEE Intern. Pulsed Power Conf. Albuquerque,* 1993, p. 511-515.
17. V.G. Artyukh, E.I. Skibenko, Yu.V. Tkach, V.B. Yuferov. *Study of a high-current plasma opening switch:* Preprint KIPT 89-28. Kharkiv: NSC KIPT, 1989.
18. V.B. Yuferov, O.S. Druj, V. G. Artyukh, V.F. Malets. Small-sized superpower pulsed electron accelerator (microwave generator) for DIN-2K irradiation // *Problems of Atomic Science and Technology. Series "Physics of Radiation Effects and Radiation Materials Science".* 1998, iss. 1(67), 2(68), p. 173-174.
19. L.A. Artsimovich, R.Z. Sagdeyev. *Plasma physics for physicists.* M.: "Atomizdat", 1979, 320 p.
20. M.V. Babykin, E.D. Volkov, P.P. Gavrin, B.A. Demidov, E.K. Zavojsky, L.I. Rudakov,

V.A. Skoryupin, V.A. Suprunenko, E.A. Sukhomlin, Ya.B. Fainberg, S.D. Fanchenko. Turbulent heating and abnormal plasma resistance. Discovery № 112 (USSR) // *Bulletin of inventions № 32*. 1972.
21. V.M. Bystritskiy, G.A. Mesyats, V.V. Kim, et al. Microsecond plasma current interrupters // *Fizika elementarnykh chastits i atomnogo yadra.* 1992, v. 23, iss. 1, p. 20-57 (in Russian).
22. G.A. Mesyats. *Ectons in vacuum discharge: breakdown, spark, arc*. M.: "Science". 2000.
23. A.E. Dubinov, I.Yu. Kornilova, V.D. Selemir. Collective ion acceleration in virtual-cathode systems. Physics-Uspekhi, 2002, iss. 11, v. 2, p. 1225-1246.
24. F.D. Huba. *Revised NRL plasma formulary*. 2000, Washington, USA.
25. E.I. Skibenko. Investigation of electron beam-generated dense plasma in a cryogenic trap with a strong magnetic field // *Ph.D. thesis*. 1972, Kharkov.
26. L.A. Artsimovich. *Controlled thermonuclear reactions.* M.: "Fizmatgiz", 1961.
27. R.F. Post. *High-temperature plasma research and controlled fusion.* M.: "Foreign literature", 1961.
28. J.B. Hasted. *Physics of atomic collisions*. M.: "Mir". 1965.
29. V.M. Zhdanov. *Transfer phenomena in a multicomponent plasma*. M.: "Ehnergoizdat", 1982.

Article received 06.06.2019

ОПРЕДЕЛЕНИЕ ЭЛЕКТРОПРОВОДНОСТИ РАЗРЯДНОГО ПРОМЕЖУТКА ПЛАЗМЕННОГО КОММУТАТОРА (ПРЕРЫВАТЕЛЯ) ТОКА

Е.И. Скибенко, А.Н. Озеров, В.Б. Юферов

Проведен анализ работы и полученных результатов генераторов импульсных токов и напряжений наносекундного диапазона с плазменными коммутаторами (прерывателями) тока ПКТ-ППТ. Расчетным путем определена электропроводимость разрядного промежутка, заполненного плазмой, в зависимости от температуры электронов плазмы, концентрации многозарядных ионов и номера их ионизационного состояния. Выделены некоторые факторы влияния плазменных свойств разрядного промежутка ПКТ-ППТ на величину электропроводности, связанные с эффективным сечением рассеяния электронов внутренним атомным полем и их столкновениями с нейтральными частицами, которые приводят к раннему снижению величины электропроводности разрядного промежутка ПКТ-ППТ до наступления фазы обрыва тока.

ВИЗНАЧЕННЯ ЕЛЕКТРОПРОВІДНОСТІ РОЗРЯДНОГО ПРОМІЖКУ ПЛАЗМОВОГО КОМУТАТОРА (ПЕРЕРИВНИКА) СТРУМУ

Є.І. Скібенко, О.М. Озеров, В.Б. Юферов

Проведено аналіз роботи і одержаних результатів генераторів імпульсних струмів і напруг наносекундного діапазону з плазмовими комутаторами (переривниками) струму ПКС-ППС. Розрахунковим шляхом визначена електропровідність розрядного проміжку, заповненого плазмою, в залежності від температури електронів плазми, концентрації багатозарядних іонів і номера їхнього іонізаційного стану. Виділені деякі фактори впливу плазмових властивостей розрядного проміжку ПКС-ППС на величину електропровідності, що зв'язані з ефективним перерізом розсіювання електронів внутрішнім атомним полем і їх зіткненнями з нейтральними частинками, які призводять до раннього зниження величини електропровідності розрядного проміжку ПКС-ППС до настання фази падіння струму.